

Study on the moisture absorption of zwitterionic copolymers for moisture-sensitive shape memory applications

Zhankui Mei^{a†}, Huanhuan Ren^{a†}, Shaojun Chen^{a*} , Zaochuan Ge^{a*} and Jinlian Hu^b



This study develops a new type of moisture-sensitive shape memory polymer based on zwitterionic copolymers synthesized with acrylic acid (AA) and 3-Dimethyl (methacryloyloxyethyl) ammonium propane sulfonate (DMAPS). The moisture absorption properties of zwitterionic copolymers are particularly investigated in this paper. The results demonstrate that the DMAPS/AA copolymers possess a sulfobetaine structure and form a two-phase separation structure. The zwitterionic copolymers show both good hydrophilic properties and moisture absorption properties. Both AA and DMAPS segments influence the hydrophilic properties and moisture absorption of the composite copolymer. The moisture absorption process is well modeled by Fick's second law in its initial stage. The moisture absorption is mainly determined by immersion conditions and the given materials' structure. Moisture absorption speed and saturated moisture absorption both increase with an increase in DMAPS content as well as the immersion temperature. The increased moisture absorption rate and higher saturated moisture absorption results from the higher activation energy of diffusion. The DMAPS/AA copolymers demonstrate adequate moisture-sensitive shape memory effects. Stain recovery is faster in the zwitterionic copolymers containing higher DMAPS content, whereas the final shape recovery decreases with an increase of DMAPS content. Finally, it is proposed that not only good moisture absorption units are required but also physical crosslinks should be improved for moisture-sensitive shape memory polymers. Copyright © 2017 John Wiley & Sons, Ltd.

Additional Supporting Information may be found online in the supporting information tab for this article.

Keywords: shape memory; smart materials; zwitterionic polymers; moisture absorption

INTRODUCTION

Zwitterionic polymers are polymers possessing both anionic and cationic groups.^[1,2] In past decades, zwitterionic polymers have been introduced for a wide variety of applications that include ion exchange, sewage treatment, chelation to bind trace metals from drinking water, soil conditioning, and paper reinforcement.^[2] Recently, polybetaines, which have the anionic and cationic groups on the same monomer units, have attracted significant interest as biomedical materials.^[1,2] They are reported to have excellent biocompatibility, show high resistance to non-specific protein adsorption, and possess suitable antimicrobial properties.^[3–6] One advantage of polybetaines for biomedical applications is that the zwitterionic groups can form a hydration layer for resisting attachment to proteins, bacteria, and blood cells. Additionally, various ionic polymers have been reported to have good moisture absorption.^[7–9] The moisture absorption and moisture absorption kinetics in polyelectrolyte films were also investigated in previous publications.^[10,11] Therefore, zwitterionic polymers might also have good moisture absorption properties. However, the moisture absorption behaviors of zwitterionic polymers are less reported in literature. It is critical to understand the moisture absorption process of zwitterionic polymers before promoting their various applications in copolymer composites.

In recent years, shape memory polymers (SMPs) are attractive to both scientists and engineers because they have the

capability of fixing a temporary shape and recovering its original shape by applying external stimuli such as heat, light, electric, and water.^[12–18] Many kinds of SMPs have been developed for various applications, including biomedical applications,^[19,20] self-healing coatings,^[21,22] actuators,^[23,24] dry adhesives,^[25] textiles,^[26,27] and information carriers.^[28,29] A conventional thermal-induced SMP relies on a reversible thermal phase transition. The thermal-induced shape fixing/recovering can be easily achieved by cooling/heating the surroundings to below/above the transition temperature. The recent development of the water-induced SMP represents an obstacle in the realization of

* Correspondence to: Shaojun Chen and Zaochuan Ge, Guangdong Research Center for Interfacial Engineering of Functional Materials; Shenzhen Key Laboratory of Polymer Science and Technology, College of Materials Science and Engineering, Shenzhen University, Shenzhen 518060, China.
E-mail: chensj@szu.edu.cn; gezc@szu.edu.cn

† Huanhuan Ren and Zhankui Mei are equal contributors to this work.

a Z. Mei, H. Ren, S. Chen, Z. Ge
Guangdong Research Center for Interfacial Engineering of Functional Materials; Shenzhen Key Laboratory of Polymer Science and Technology, College of Materials Science and Engineering, Shenzhen University, Shenzhen 518060, China

b J. Hu
Institute of Textiles and Clothing, the Hong Kong Polytechnic University, Hung Hum, Kowloon, Hong Kong

its full potential for practical applications without the need of heat stimuli.^[30,31] Another route for shape recovery is by reducing the thermal phase transitions below the surrounding temperature with the stimulus of water, moisture, chemistry, and so on.^[30,31] Since the first report of water-driven programmable shape memory polyurethane in 2005,^[32] non-thermally induced SMPs have rapidly become investigated. Recently, Wang *et al.* investigated the water-induced shape memory effect (SME) in sodium dodecyl sulfate/epoxy composites.^[33] Lu *et al.* also reported the chemo-responsive SME in shape memory polyurethane triggered by inductive release of mechanical energy storage via copper (II) chloride migration.^[34] By utilizing the features of thermo/moisture-responsive SMPs, Sun *et al.* proposed a concept of incorporating micro-sized devices made of SMPs that were delivered into living cells for surgery or operation.^[35] However, the biocompatibility should first be considered before promoting these SMPs for biomedical applications. Even though most zwitterionic polymers are reported to show good biocompatibility, there are few reports on zwitterionic SMPs.^[1,2] Zwitterionic polymers provide a feasible way to achieve both good biocompatibility and moisture-sensitive SMEs. The moisture-sensitive SMEs of zwitterionic polymers might greatly promote the biomedical application of SMPs.

In previous publications, we developed a new kind of moisture-sensitive SMP from the pyridine-containing polyurethane.^[36,37] The mechanism of moisture-sensitive SMEs could be ascribed to the dissociation of hydrogen bonding presented in the pyridine ring because of moisture absorption.^[36] Thus, moisture absorption behavior plays an important role in the moisture-sensitive SME. Most recently, we successfully developed zwitterionic SMPs synthesized with acrylic acid (AA) and 3-Dimethyl (methacryloyloxyethyl) ammonium propane sulfonate (DMAPS). Preliminary results demonstrate that the DMAPS/AA copolymers were found to show not only multi-SME and moisture-sensitive SME properties but also good biocompatibility.^[38] However, the moisture absorption of zwitterionic polymers and the moisture absorption kinetics have not been investigated until now. Therefore, on basis of the analysis of structure and morphology, we have carefully investigated the hydrophilic properties, moisture absorption, moisture absorption kinetics, and moisture-sensitive SMEs in this study.

EXPERIMENT

Materials

Sodium hydroxide (NaOH), ammonium persulphate ((NH₄)₂S₂O₈), acrylic acid (AA, cat.#174230), and other common chemicals were purchased from Aladdin (Shanghai, China). 3-Dimethyl (methacryloyloxyethyl) ammonium propane sulfonate (DMAPS, ca.#537284) was synthesized by Changzhou Yipingtang Co. Ltd. (Changzhou, China).

Synthesis of DMAPS/AA copolymers

The DMAPS/AA copolymers with various DMAPS content were synthesized with DMAPS and AA via a free-radical polymerization method according to the procedure in our previous publication.^[38] The reaction was performed in a nitrogen-filled three-neck flask with mechanical stirring. Firstly, the monomers, DMAPS and AA, were added to the flask, the polymerization was initiated with addition of (NH₄)₂S₂O₈ into the solution, and

the reaction was kept at 60°C for 10 hr. Finally, a 10 wt% polymer solution was obtained. DMAPS/AA copolymer samples could be obtained by heating a Teflon pan of the polymer solution at 80°C for 24 hr in continuous air flow and then *in vacuo* for another 24 hr. In this study, the samples were labeled as DMAPS##, in which ## is the weight fraction of DMAPS.

Materials characterizations

Fourier transformation infrared (FT-IR) spectra were obtained with an FT-IR spectrometer (Nicolet 6700, Nicolet, USA) equipped with an Attenuated total reflection (ATR) accessory; 24 scans at a 4-cm⁻¹ resolution were signal averaged and stored as data files for further analysis.

Dynamic mechanical analysis (DMA) curves were determined using a Q200 instrument (TA, USA) purged with nitrogen, while operating at a heating rate of 2°C/min from -60°C to 180°C and at 1 Hz. The specimens for testing were prepared by casting a film of thickness of 0.5 mm, a length of 25 mm, and a width of 5 mm.

X-ray photoelectron spectroscopy (XPS) spectra were recorded on a VG multilab2000 with Al K_α source. The anode current was 10 mA, and the anode voltage was at 15 KV. The core-level signals were obtained at a photoelectron take-off angle of 90°. The elemental compositions were obtained from peak areas and sensitivity factor from the C_{1s}, O_{1s}, N_{1s}, and S_{2p} peaks by TA advantage software. All binding energies were calculated in reference to carbon, C1s = 284.6 eV.

Static contact angle of samples were investigated with a JC2000Y stable contact angle analyzer (Chengde Chengwei Tester Co. Ltd., Chengde, China) by using distilled water as the test liquid.

Characterization for moisture absorption

The moisture absorption was determined by weighing method described in previous publications.^[37,39] Before testing, the specimens were completely dried. The specimen was then put on the moisture condition at a specific temperature and a certain RH for moisture absorption (Fig. S1). For example, on the first stage, the duration of moisturizing time is short (e.g. ΔT = 5 min). After 30 min, the duration is gradually increased (e.g. ΔT = 10 min) on the second stage. After 2 hr, the duration time is further prolonged (e.g. ΔT = 30 min or 60 min) before the weight of specimen is determined to be relatively constant. The measuring time is about 5 min. Finally, the moisture absorption in percentage at any time (M_t) is calculated by the following equation:^[39]

$$M_t = [(W_t - W_d)/W_d] \times 100\% \quad (1)$$

where W_d and W_t refer to the weight of the dry specimen and the wet specimen, respectively.

Kinetics of moisture absorption

The kinetics of moisture absorption was studied according to the method previously described in literature.^[37,40-42] Diffusion is a thermally activated process, and the diffusion coefficient obeys the classical transition state theory, and its temperature dependence can be expressed by the Arrhenius equation (eqn 2):^[42]

$$D = D_0 e^{-E_a/RT} \quad (2)$$

in which D₀ is the maximum diffusion coefficient (at infinite temperature), E_a is the activation energy of diffusion, and R is

the gas constant. In contrast to the diffusivity, water absorption into a polymer is modeled as a Fickian process for the time resolved mass increase for a thin film on an impermeable substrate. Thus, the mass gains at any time could be expressed with the following equation (as seen in eqn 3):^[42]

$$\frac{M_t}{M_\infty} = 2 \left(\frac{D_t}{h^2} \right)^{0.5} \left(\frac{1}{\pi^{0.5}} + 2 \sum_{n=1}^{\infty} (-1)^n \operatorname{ierfc} \frac{nh}{2(D_t)^{0.5}} \right) \quad (3)$$

where M_t and M_∞ are the mass gains at time t and at equilibrium, respectively. D is the diffusivity, and h is the thickness of tested film. The penetrate absorption is assumed to be one-dimensional because of the large surface area to volume ratio and the impermeable substrate. At short times, this expression can be simplified to eqn 4:^[42]

$$\frac{M_t}{M_\infty} = \frac{2}{h} \sqrt{\frac{D_t}{\pi}} \quad (4)$$

According to eqn 2 and 4, the dependency of M_t on time can be expressed with eqn 5:

$$\frac{M_t}{M_\infty} = \frac{2}{h} \left[\left(D_0 e^{(-E_a/RT)} \frac{t}{\pi} \right) \right]^{1/2} \quad (5)$$

At lower RH, sorption of gasses and vapors into glassy polymers is successfully described by a dual-mode sorption theory. The equilibrium component of the theory is expressed with eqn 6:^[42]

$$C = K_D P + C_H' b P / (1 + b P) \quad (6)$$

where C is the total solubility in polymer, P is the pressure related to the RH, K_D is Henry's law dissolution constant, b is the hole affinity constant in polymer, and C_H' is the hole saturation constant in polymer. According to the eqn 5, the dependency of M_t on time can be expressed with eqn 7:^[42]

$$\begin{aligned} \ln M_t = & 0.5 \ln 2/h + .5 \ln D_0 - 0.5 \ln \delta \\ & + \ln M_\infty - 0.5 E_a/RT + 0.5 \ln t \end{aligned} \quad (7)$$

For the same sample, the eqn 7 can be simplified to eqn 8:

$$\ln M_t = C + \ln M_\infty - 0.5 E_a/RT + 0.5 \ln t \quad (8)$$

$$\text{where } C = 0.5 (\ln 2/h + \ln D_0 - \ln \delta) \quad (9)$$

At a certain temperature, the eqn 8 can be simplified to eqn 10.

$$\ln M_t = K + 0.5 \ln t \quad (10)$$

$$\text{where } K = C + \ln M_\infty - 0.5 E_a/RT \quad (11)$$

The eqn 11 can be further expressed with eqn 12:

$$K = C' - 0.5 E_a/RT \quad (12)$$

$$\text{in which } C' = C + \ln M_\infty \quad (13)$$

$$\text{Thus, } dK/d_{1/T} = -0.5 E_a/R \quad (14)$$

RESULTS AND DISCUSSION

Structure and morphology analysis

In this experiment, the zwitterionic copolymer was synthesized directly with AA and DMAPS via a free-radical polymerization method.^[38] The structure and morphology were firstly analyzed via FT-IR, XPS, and DMA. FT-IR spectra demonstrate that the vibration frequencies of SO_3^- groups at 1038 cm^{-1} and ammonium groups at 960 cm^{-1} appear in the DMAPS and the obtained samples (Fig. 1). As the DMAPS content increases, the frequency at 1710 cm^{-1} (e.g. in DMAPS20) shifts to 1719 cm^{-1} (e.g. in DMAPS60 and pure DMAPS). This frequency should be attributed to the stretching vibration of C=O in the DMAPS segment. As the AA content decreases, the presence of the C=O stretching vibration at 1645 cm^{-1} in sample DMAPS60 shifts to 1637 cm^{-1} for sample DMAPS20. The intensity at this frequency also increases with an increase in AA segments; thus, this vibration frequency should be ascribed to the AA segment. This result suggests that the DMAPS is copolymerized with AA to successfully yield zwitterionic copolymers. Additionally, the XPS survey scan spectra demonstrate that S_{2p} (binding energy, 166 eV) and N_{1s} (binding energy, 400 eV), which are two indicative atoms for DMAPS, are detected in the DMAPS/AA copolymers. Furthermore, the N_{1s} spectrum consists of two peaks, one peak at 402 eV for the sulfobetaine ammonium nitrogen ($-\text{N}^+(\text{CH}_3)_2\text{CH}_2$) and the other peak at 400 eV for the nitrogen in the residues of the NH_4^+ cations from $(\text{NH}_4)_2\text{S}_2\text{O}_8$ serving as the initiator because ammonium nitrogen was only measured in the N_{1s} spectrum of pure DMAPS (Fig. 2). It is thus confirmed that the DMAPS/AA copolymers possess the sulfobetaine structure. This sulfobetaine might provide the structural foundation for good biocompatibility critical for many biomedical applications.^[43] Additionally, the AA segment also contains carboxylic acid groups that form hydrogen bonds and allow for moisture sensitivity. Moreover, the strong hydrogen bonds among AA segments might serve as reversible switches while the strong electrostatic forces among DMAPS segments could serve as physical netpoints for the composite copolymer. Thus, results suggest that a two-phase separation structure might be formed in the DMAPS/AA copolymers.

Morphology of DMAPS/AA copolymers was investigated with DMA measurements. The DMA curves of samples DMAPS20 and DMAPS50 demonstrate that the zwitterionic copolymers have high storage modulus in their glassy state and a lower storage modulus in their rubbery state. Significant decrease in modulus is observed in all DMAPS/AA copolymers that suggest that the formation of an amorphous soft phase in the copolymer. The glass transition temperature (T_g) also shifts to a higher temperature range as the DMAPS content increases, suggesting the reinforcement of DMAPS segment (Fig. 3). Even though the rubbery modulus gradually decreases with an increase in temperature, the rubbery modulus is higher than 10 MPa below 100°C , suggesting good stiffness within a high temperature range because of the good physical crosslinks. $\tan \delta$ curves further demonstrate that both samples exhibit two peaks, resulting from the glass transition of the soft and hard phases (Fig. 3); thus, these findings confirm the formation of a two-phase separation structure. A hypothesis is that the hard phase might be formed with the aggregated zwitterionic DMAPS segments, while the amorphous soft phase is greatly influenced by the hydrogen bonding of AA segments. The $\tan \delta$ peak attributed to hard segments shifted to high temperature side in DMAPS50 sample,

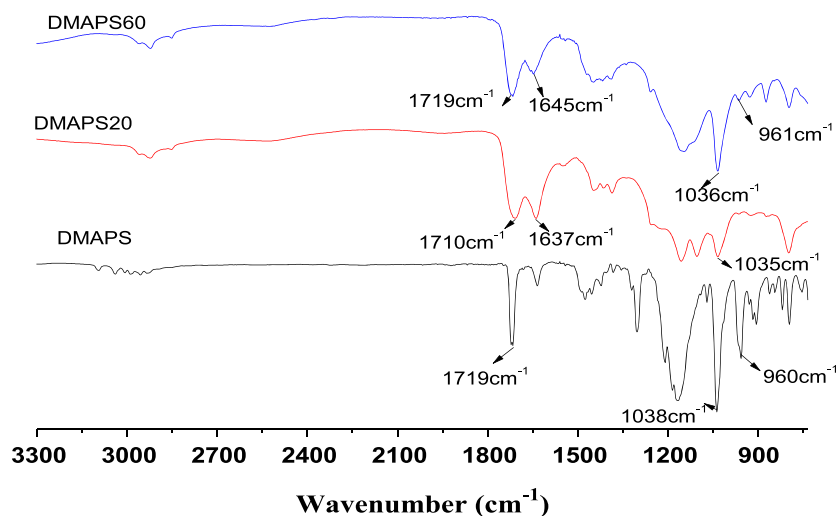


Figure 1. Fourier transformation infrared spectra of DMAPS/AA copolymer. [Colour figure can be viewed at wileyonlinelibrary.com]

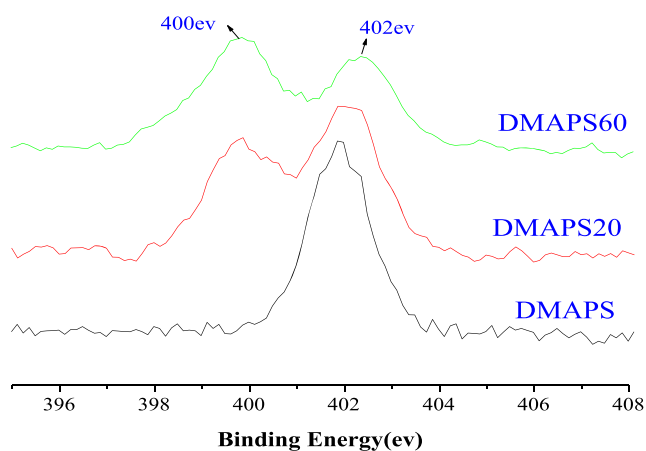


Figure 2. X-ray photoelectron spectroscopy spectra of DMAPS/AA copolymers. [Colour figure can be viewed at wileyonlinelibrary.com]

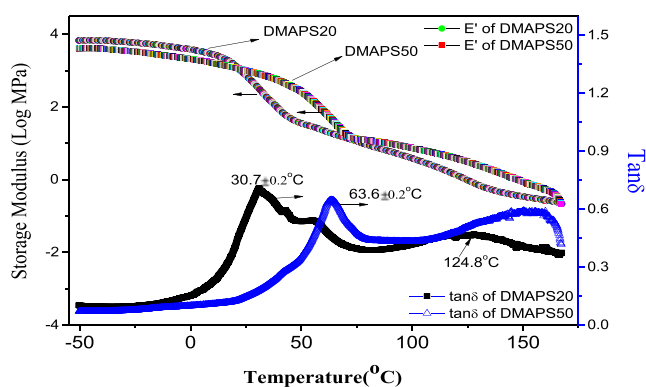


Figure 3. Dynamic mechanical analysis curves of typical DMAPS/AA copolymers. [Colour figure can be viewed at wileyonlinelibrary.com]

confirming more aggregation of zwitterionic DMAPS segments. Differential Scanning calorimeter (DSC) curves further confirm that the DMAPS/AA copolymers have amorphous soft phase, in which the T_g increases with the increase of DMAPS

content (Fig. S3). This structure and morphology satisfy the pre-condition for good shape memory properties of DMAPS/AA copolymers.^[12]

Hydrophilic properties

The incorporation of sulfobetaine structure is hypothesized to affect the hydrophilic properties of zwitterionic copolymers. Figure 4A presents a representative water contact angle of sample DMAPS60. The water contact angle is relatively high in sample DMAPS20, suggesting poor hydrophilic properties; whereas the water contact angle decreases as the DMAPS content increases (Fig. 4B). This finding indicates that the hydrophilic properties of zwitterionic copolymers are primarily determined by the DMAPS segments. When sample DMAPS50 was adjusted with NaOH to a different pH value, the hydrophilic properties were significantly altered. Figure 4C illustrates the dependence of water contact angle on pH value. As the pH value increases, the water contact angle increases, suggesting a marked decrease in hydrophilicity. A possible reason is that a fraction of the hydrogen bonds among AA segments are disrupted by increasing the pH value. The disrupted hydrogen bonds are no longer capable of attracting water molecules, which effectively results in a decrease in the copolymer's hydrophilic properties. It is thus confirmed that both sulfobetaine structure and hydrogen bonding among AA segments provides hydrophilic properties to the zwitterionic copolymers. The hydrophilic properties might promote the formation of a hydration layer, which is thought to be responsible for their excellent biocompatibility and good moisture absorption properties.

Moisture absorption behavior

Moisture absorption in polymers is vital for a variety of industries ranging from microelectronics to adhesives and coatings.^[44] Aiming at a complete understanding of the moisture-sensitive SME of zwitterionic copolymers, it is necessary to study their moisture absorption behavior. In this study, the moisture absorption was determined by weighing the specimens on a balance. The moisture absorption in percentage at any given time (M_t)

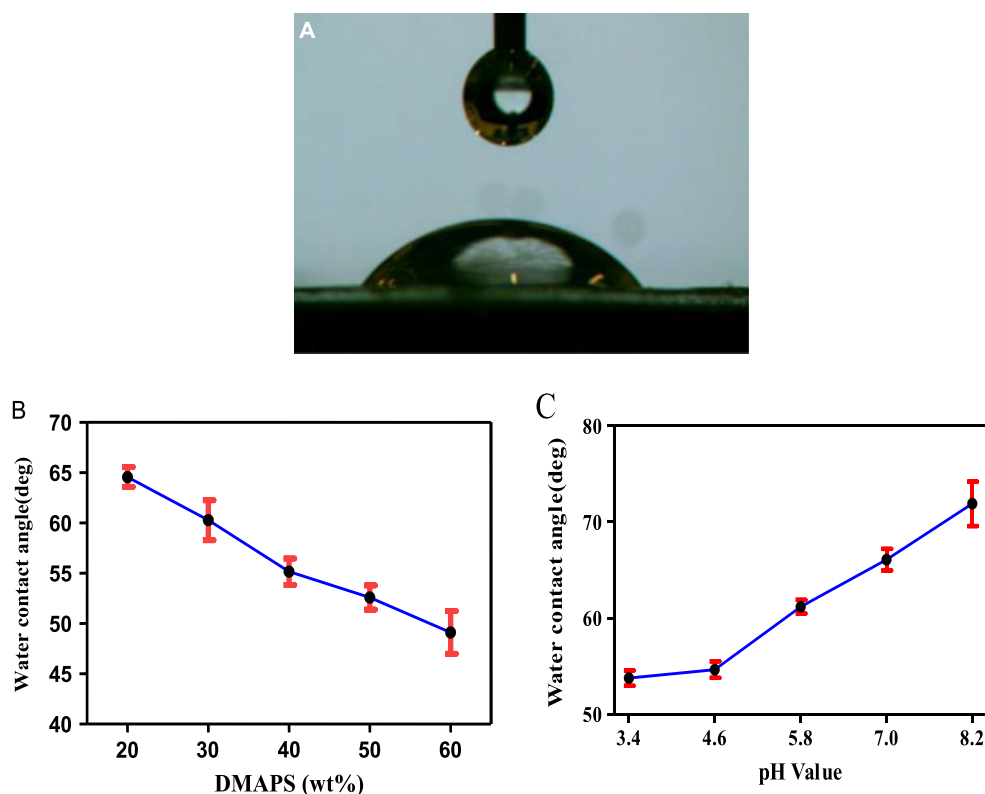


Figure 4. Hydrophilic properties of zwitterionic copolymers [(A) representative water contact angle; (B) dependency of water contact angle on DMAPS content; (C) dependency of water contact angle on pH value for sample DMAPS50]. [Colour figure can be viewed at wileyonlinelibrary.com]

could be calculated using eqn 1. The moisture absorption curves of zwitterionic copolymers of varying DMAPS content are presented in Fig. 5A. These curves clearly depict the moisture absorption process. All samples absorb moisture very quickly within the first 40 min yet then appear to slow down and tend to reach its saturated state after 200 min under the moisture conditions of 80% RH within the temperature range of 20°C–60°C. This curve indicates that the moisture absorption process of zwitterionic copolymers is well modeled by Fick's second law in its initial stage.^[44,45] In addition, the curves clearly show

the effect of DMAPS content on the moisture absorption of zwitterionic copolymers. Even though all samples exhibit identical moisture absorption processes, the M_t tends to be higher in the samples with higher DMAPS content (Fig. 5A). Figure 5B further demonstrates that the saturated moisture absorption linearly increases with an increase of DMAPS content in the zwitterionic copolymers. This result indicates that DMAPS content has a strong contribution to the moisture absorption. The zwitterionic structure might be responsible for moisture absorption properties of zwitterionic copolymers.

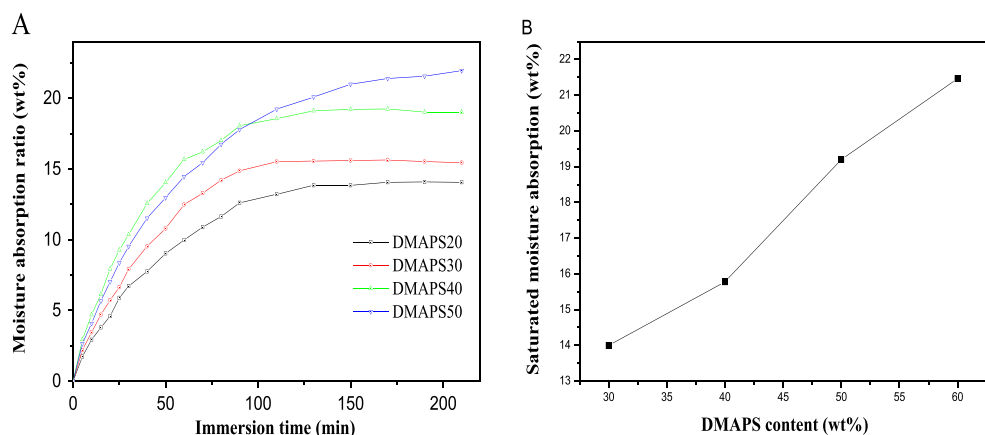


Figure 5. Moisture absorption of zwitterionic copolymers of varying DMAPS content under 80% RH and $T = 30^\circ\text{C}$ [(A) moisture absorption curves; (B) dependency of saturated moisture absorption on DMAPS content]. [Colour figure can be viewed at wileyonlinelibrary.com]

The effect of the immersion temperature was also investigated in this investigation. Figure 6 presents the moisture absorption of sample DMAPS60 under a moisture condition at varying temperature and a constant RH (RH = 80%). Figure 6A demonstrates that all moisture absorption curves exhibit a similar initial slope that suggests an identical absorption rate on the surface of the polymeric film. However, M_t at higher temperatures is generally higher than those at lower temperatures, which is indicative of the solubility of water being higher at a higher immersion temperature. Additionally, Fig. 6B also demonstrates that the saturated moisture absorption increases in a linear behavior with an increase of temperature in particular within the temperature range of 20°C–50°C. Previously reported in literature, it was revealed that the solubility of water in semi-crystalline poly(ester urethane) increases with an increase of immersion temperature.^[46] This is because the diffusion rate is the primary driving force to the moisture absorption in the bulk polymeric materials, in which the diffusion coefficient increases with increasing immersion temperature. In the same materials' structure, the higher diffusion coefficient will greatly promote the movement of absorbed water molecules from the surface to the bulk of the polymer, improving the solubility of water in the composite. This finding confirms that the moisture absorption of polymer is primarily determined by the immersion conditions and materials' structure. In comparison with previous polymer systems like pyridine-containing polyurethane^[37] and semi-crystalline poly(ester urethane),^[46] the zwitterionic copolymer in this study demonstrates not only a much higher saturated moisture absorption but also faster absorption rate. This might be the most important feature for zwitterionic copolymers that demonstrate good moisture-sensitive SME.

Kinetics of moisture absorption

Aiming at a deeper understanding of the mechanism of moisture absorption of zwitterionic copolymers, the moisture absorption kinetics of zwitterionic copolymers is also investigated in this study. The calculation for moisture absorption kinetics was described in Section 2.4. As described previously, a good linear relationship between saturated moisture

absorption and immersion temperature was found within the temperature range of 20–50°C. Thus, the moisture absorption behaviors are investigated at the constant moisture condition of 80% RH while the immersion temperature is varied from 25°C to 50°C. Figure 7 displays the dependency of moisture absorption on immersion time for sample DMAPS60. According to the calculation method of kinetics,^[37,42] the relationship between $\ln M_t$ and $0.5\ln t$ could be obtained, as shown in Fig. 8. Figure 8 confirms that the moisture absorption of zwitterionic copolymers are well modeled by Fick's second law because they show a good linear relationships in their initial state^[47]. According to Fig. 8, the K value at different temperatures (T) can be calculated from the intercept of Fig. 8, in which the dependency of K on $1/T$ is shown in Fig. 9. According to Fig. 9, the slope of the fitted line and its intercept are -3283 and 14.1 , respectively. Thus, by using eqn 12, the activation energy of diffusion E_a can be calculated with the use of $R = 8.31 \text{ J mol}^{-1} \text{ K}^{-1}$. The constant C' in eqn 12 exactly corresponds to the intercept,^[42] i.e.

$$E_a = 54.5 \text{ KJ mol}^{-1} \text{ and } C' = 14.1$$

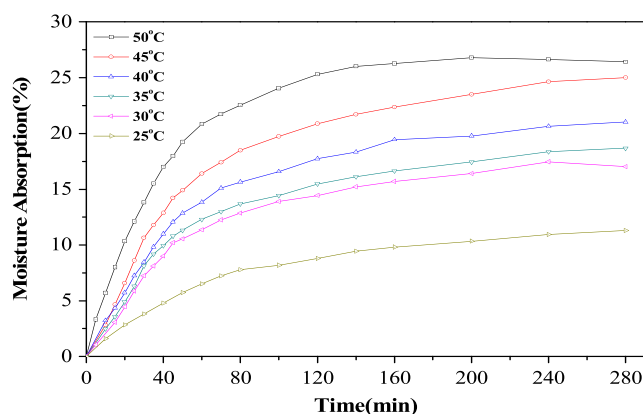


Figure 7. Dependency of moisture absorption of sample DMAPS60 at the moisture condition of RH80% and different temperatures. [Colour figure can be viewed at wileyonlinelibrary.com]

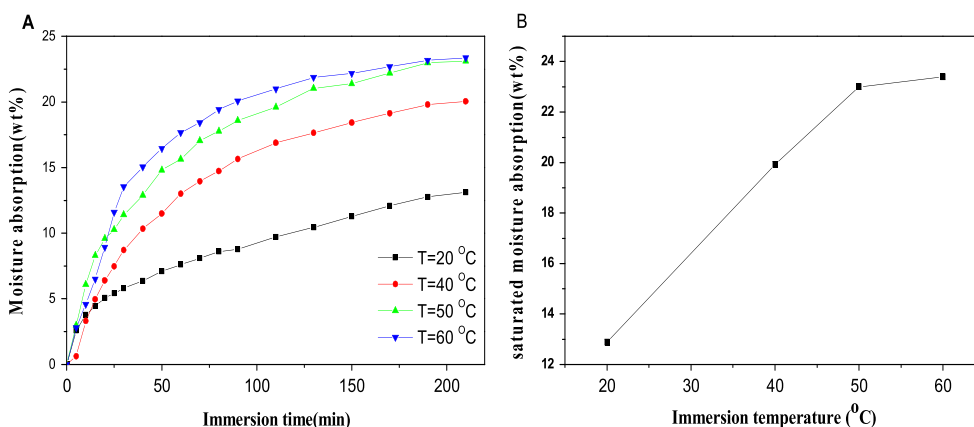


Figure 6. Moisture absorption of sample DMAPS60 under 80 RH% as a function of temperature [(A) moisture absorption curves; (B) saturated moisture absorption at different temperature]. [Colour figure can be viewed at wileyonlinelibrary.com]

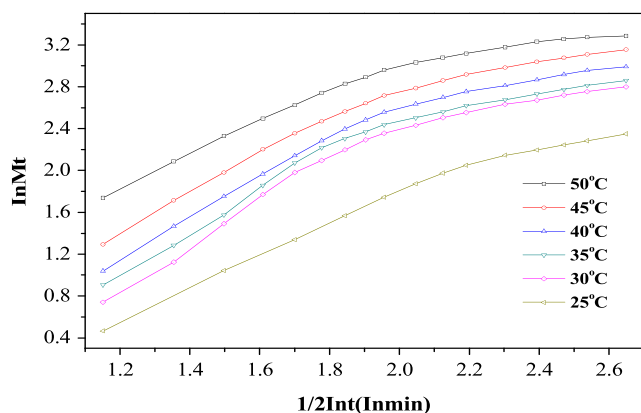


Figure 8. Dependency of $\ln M_t$ on 0.5Int . [Colour figure can be viewed at wileyonlinelibrary.com]

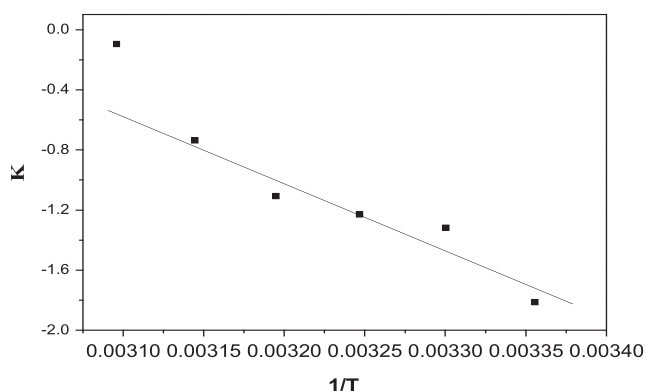


Figure 9. Dependency of K on $1/T$.

By assuming that M_∞ is independent of temperature, $\ln M_\infty = 3.27$ can be calculated from Fig. 7 when $M_\infty = 26.3$ is the saturated moisture absorption at 50°C .

According to eqn 8, the constant C in eqn 8 is calculated with the use of $\ln M_\infty$, i.e.

$$C = -10.83$$

In addition, the thickness of the testing film in this experiment is about 1.0 mm, i.e. $h = 1.0$ mm. Using eqn 9, the maximum diffusion coefficient D_0 can be effectively obtained, i.e.

$$D_0 = 1.63 \times 10^{10} \text{ m}^2/\text{s}$$

Finally, the relationship between moisture absorption at a given time (M_t) and time (t) at various temperatures (T) for sample DMAPS60 under the moisture condition of 80%RH can be expressed by the following equation (eqn 15):

$$\ln M_t = 14.1 - 3283(1/T) + 0.5 \text{Int} \quad (15)$$

Therefore, moisture absorption kinetics confirms that the moisture absorption process of zwitterionic copolymers can be successfully modeled by Fick's second law in its initial stage. As compared with the previously reported pyridine-containing polyurethane,^[37] the activation energy of zwitterionic copolymer is much higher. This higher activation energy of diffusion is the basic reason for their high moisture absorption speed and higher saturated moisture absorption. These findings convince us that the zwitterionic copolymer demonstrates good moisture-sensitive SME with a fast strain recovery speed.

Moisture-sensitive SMEs

On basis of the aforementioned analysis, the structure and morphology of zwitterionic copolymers effectively satisfies the fundamental structural requirements for polymers exhibiting SMEs; moreover, the copolymers exhibit good moisture absorption properties. Therefore, the DMAPS/AA copolymers are expected to show good moisture-sensitive SME. In this experiment, the moisture-sensitive SME is investigated from the strain recovery, recovery immersion time and recovery speed according to the method previously described in literature.^[36] Firstly,

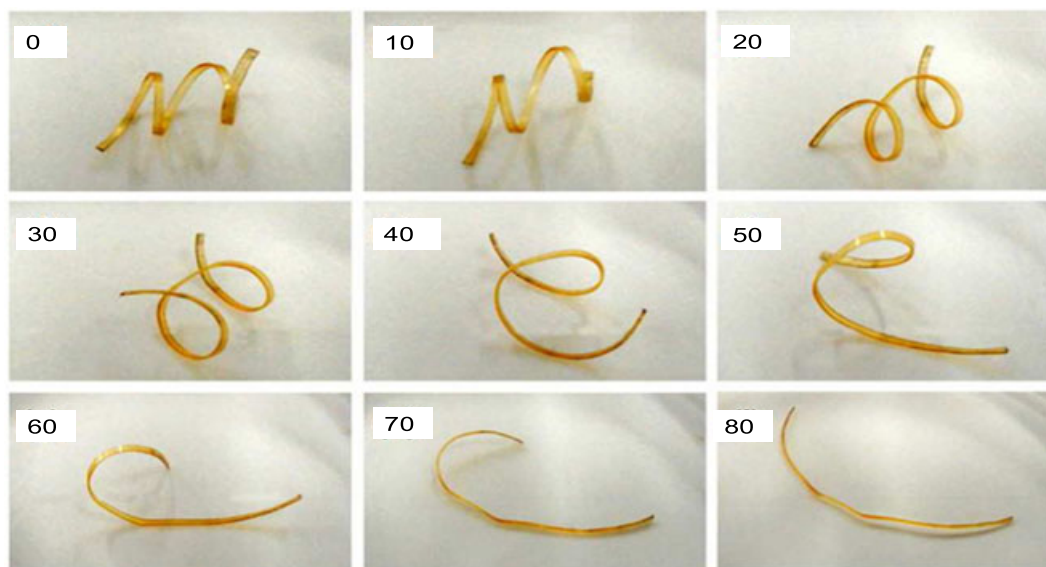


Figure 10. Images showing typical moisture-sensitive shape recovery process. [Colour figure can be viewed at wileyonlinelibrary.com]

the specimen is deformed to a second temporary shape by external force and fixed at room temperature. After the fixed temporary shape is exposed to a moisture condition of RH = 80% at $T = 30^{\circ}\text{C}$, the specimen can be found to recover itself. The strain recovery started at about 30 min of immersion time. Significant strain recovery was observed within the immersion time range of 30–60 min. Beyond 60 min, the original shape was completely recovered (Fig. 10). Similar to the thermal-induced SMEs as described in literature,^[48] the moisture-sensitive strain recovery process is also characterized with several parameters, such as strain recovery start time (t_s), strain recovery time (t_r), strain recovery end time (t_e), immersion time length (Δt), and final strain recovery (R_r).^[36] The more detailed calculations can be found in Fig. S2. The variables are as follows: t_s is defined as the immersion time at which the strain recovery is about 10% R_r , t_r is defined as the immersion time at which the strain recovery is about 50% R_r , t_e is defined as the immersion time at which the strain recovery is about 90% R_r , and Δt ($\Delta t = t_e - t_s$) is also used to characterize the strain recovery speed.^[36] Table 1 summarizes the parameters of moisture-sensitive strain recovery for DMAPS/AA copolymers of varying DMAPS content. For investigating the relationship between strain recovery and moisture absorption, the saturated moisture absorption for each sample is also provided. Table 1 demonstrates that all immersion times including t_s , t_r , t_e , and Δt decrease as the DMAPS content increases. Meanwhile, the saturated moisture absorption increases with the increase of DMAPS content. This result suggests that strain recovery is faster in the samples with higher DMAPS content because of their higher moisture absorption rate, as described previously. On the contrary, R_r decreases with an increase of DMAPS content. A possible reason should be ascribed to their higher saturated moisture absorption. An excess amount of water molecules might impede hydrogen bonding and aggregation of zwitterionic segments in the zwitterionic copolymer, effectively decreasing the physical netpoints, further influencing the total strain recovery. This observation was also found in the moisture-sensitive SME of pyridine-containing polyurethane in a previous investigation. As compared with the polyurethane system, the DMAPS/AA copolymer shows fast strain recovery speed under the moisture condition because of their sulfobetaine structure and hydrogen bonding as mentioned previously. The strain recovery decreases with the increase of DMAPS content in DMAPS/AA copolymers, whereas the strain recovery is higher in the polyurethane with high content of pyridine ring. This quite difference should be resulted from their different physical crosslinks. The strong hydrogen bonding between urethanes serves as physical netpoints in the polyurethane while the electrostatic force between DMAPS segments serves as physical netpoints in DMAPS/AA

copolymers. It is thus proposed that not only a high fraction of moisture absorption units is required but also physical crosslinks should be improved in the molecular designing of moisture-sensitive SMPs.

CONCLUSIONS

This study develops a new kind of moisture-sensitive SMPs based on a zwitterionic copolymer synthesized with DMAPS and AA segments. In order to understand the moisture-sensitive SME of zwitterionic copolymers, the structure and morphology, hydrophilic properties, moisture absorption, and moisture absorption kinetics were carefully investigated in this paper. The results demonstrate that the DMAPS/AA copolymers possess a sulfobetaine structure and form a two-phase separation structure. The zwitterionic polymers show both good hydrophilic properties and moisture absorption properties across varying DMAPS content, in which both AA and DMAPS segments contribute to the hydrophilic properties. The moisture absorption behavior is primarily determined by immersion conditions and the materials' structure. Both moisture absorption rate and saturated moisture absorption increase with an increase of DMAPS content and the immersion temperature. Moisture absorption kinetics further confirms that the moisture absorption process is well modeled by Fick's second law during the initial stage. The higher activation energy of diffusion is the elementary mechanism that contributes to the copolymers' high moisture absorption rate and saturated moisture absorption. Additionally, the DMAPS/AA copolymers exhibit good moisture-sensitive SME. Strain recovery is faster in the zwitterionic copolymers with higher DMAPS content, whereas R_r decreases with an increase of DMAPS content. It is thus proposed that not only good moisture absorption units are required but also netpoints should be improved for moisture-sensitive SMPs.

Acknowledgements

The authors gratefully acknowledge the financially supported by the Natural Science Foundation of Guangdong (Grant Nos. 2014A030313559, 2014A030311028, 2016A030313050), the Nanshan District Key Lab for Biopolymers and Safety Evaluation (No. KC2014ZDZJ0001A), the Science and Technology Project of Shenzhen City (Grant Nos. JCYJ20140828163633993, JCYJ20140828163633993, XCL201110060, ZDSYS20140430164 957665, ZDSYS201507141105130), and the Hong Kong Research Grants Council projects (RGC-GRF/5161/11E, RGC-GRF/5162/12E).

CONFLICTS OF INTEREST

The authors declare no conflict of interest.

REFERENCES

- [1] F. Xuan, J. Liu, *Polym. Int.* **2009**, *58*, 1350.
- [2] A. B. Lowe, C. L. McCormick, *Chem. Rev.* **2002**, *102*, 4177.
- [3] J. Baggerman, A. T. Nguyen, J. M. J. Paulusse, C. J. M. Van Rijn, H. Zuilhof, *Langmuir* **2011**, *27*, 2587.
- [4] S. G. Chen, S. J. Chen, S. Jiang, Y. M. Mo, J. N. Tang, Z. C. Ge, *Surf. Sci.* **2011**, *605*, L25.
- [5] R. Lalani, L. Liu, *Biomacromolecules* **2012**, *13*, 1853.
- [6] F. Cao, L. Tan, L. Xiang, S. Liu, Y. Wang, *J. Biomat. Sci. Polym. E.* **2013**, *24*, 2058.

Table 1. Parameters of moisture-sensitive strain recovery for zwitterionic copolymers

Sample	t_s (min)	t_r (min)	t_e (min)	Δt (min)	R_r (%)	W_{sma}
DMAPS20	63	90	126	63	93	14.0
DMAPS30	55	46	105	50	91	15.5
DMAPS40	35	55	82	47	89	19.0
DMAPS50	27	45	70	43	84	22.0

W_{sma} is the saturated moisture absorption.

- [7] J. Restolho, J. L. Mata, R. Colaco, B. Saramago, *J. Phys. Chem. C* **2013**, *117*, 10454.
- [8] R. L. Jia, S. M. Dong, T. Hasegawa, J. P. Ye, R. H. Dauskardt, *Int. J. Hydrogen Energy* **2012**, *37*, 6790.
- [9] C. P. L. Rubinger, C. R. Martins, M. A. De Paoli, R. M. Rubinger, *Sensor. Actuat. B. Chem.* **2007**, *123*, 42.
- [10] B. D. Vogt, C. L. Soles, H. J. Lee, E. K. Lin, W. L. Wu, *Langmuir* **2004**, *20*, 1453.
- [11] M. Bajpai, S. K. Bajpai, P. Jyotishi, *Int. J. Biol. Macromol.* **2016**, *84*, 1.
- [12] Q. Zhao, H. J. Qi, T. Xie, *Prog. Polym. Sci.* **2015**, *49-50*, 79.
- [13] M. D. Hager, S. Bode, C. Weber, U. S. Schubert, *Prog. Polym. Sci.* **2015**, *49-50*, 3.
- [14] Y. J. Liu, H. Y. Du, L. W. Liu, J. S. Leng, *Smart Mater. Struct.* **2014**, *23*, 023001.
- [15] I. A. Rousseau, *Polym. Eng. Sci.* **2008**, *48*, 2075.
- [16] T. Pretsch, *Polymers-Basel* **2010**, *2*, 120.
- [17] L. Sun, W. M. Huang, Z. Ding, Y. Zhao, C. C. Wang, H. Purnawali, C. Tang, *Mater Design* **2012**, *33*, 577.
- [18] K. S. S. Kumar, R. Biju, C. P. R. Nair, *React. Funct. Polym.* **2013**, *73*, 421.
- [19] M. C. Serrano, G. A. Ameer, *Macromol. Biosci.* **2012**, *12*, 1156.
- [20] A. Lendlein, M. Behl, B. Hiebl, C. Wischke, *Expert Rev. Med. Devices* **2010**, *7*, 357.
- [21] X. F. Luo, P. T. Mather, *ACS Macro Lett.* **2013**, *2*, 152.
- [22] D. Wang, J. Guo, H. Zhang, B. C. Cheng, H. Shen, N. Zhao, J. Xu, *J. Mater. Chem. A* **2015**, *3*, 12864.
- [23] Y. Zhao, L. Song, Z. P. Zhang, L. T. Qu, *Energ. Environ. Sci.* **2013**, *6*, 3520.
- [24] M. Bothe, T. Pretsch, *J. Mater. Chem. A* **2013**, *1*, 14491.
- [25] J. Eisenhaure, S. Kim, *Polymer* **2014**, *6*, 2274.
- [26] J. Hu, S. Chen, *J. Mater. Chem.* **2010**, *20*, 3346.
- [27] J. L. Hu, H. P. Meng, G. Q. Li, S. I. Ibeke, *Smart Mater. Struct.* **2012**, *21*, 2440.
- [28] M. Ecker, T. Pretsch, *RSC Adv.* **2014**, *4*, 286.
- [29] M. Ecker, T. Pretsch, *RSC Adv.* **2014**, *4*, 46680.
- [30] Y. C. Jung, H. H. So, J. W. Cho, *ICAFPM 2005* **2005**, *1*, 954.
- [31] X. Gu, P. T. Mather, *RSC Adv.* **2013**, *3*, 15783.
- [32] W. M. Huang, B. Yang, L. An, C. Li, Y. S. Chan, *Appl. Phys. Lett.* **2005**, *86*.
- [33] W. Wang, H. Lu, Y. Liu, J. Leng, *J. Mater. Chem. A* **2014**, *2*, 5441.
- [34] H. B. Lu, C. R. Lu, W. M. Huang, J. S. Leng, *Smart Mater. Struct.* **2015**, *24*, 035018.
- [35] L. Sun, W. M. Huang, *Mater. Design* **2010**, *31*, 2684.
- [36] S. J. Chen, J. L. Hu, S. G. Chen, *Polym. Int.* **2012**, *61*, 314.
- [37] S. J. Chen, J. L. Hu, H. T. Zhuo, *J. Mater. Sci.* **2011**, *46*, 6581.
- [38] S. J. Chen, F. N. Mo, F. J. Stadler, S. G. Chen, Z. C. Ge, H. T. Zhuo, *J. Mater. Chem. B* **2015**, *3*, 6645.
- [39] S. T. Li, L. Liang, J. Y. Li, N. J. Liu, M. A. Alim, *Mater. Lett.* **2006**, *60*, 114.
- [40] Y. Z. Wan, Y. L. Wang, H. L. Luo, X. H. Dong, G. X. Cheng, *Mat. Sci. A-Struct.* **2002**, *326*, 324.
- [41] S. Panthapulakkal, M. Sain, *J. Compos. Mater.* **2007**, *41*, 1871.
- [42] L. R. Bao, A. F. Yee, *Polymer* **2002**, *43*, 3987.
- [43] J. T. Sun, Z. Q. Yu, C. Y. Hong, C. Y. Pan, *Macromol. Rapid Commun.* **2012**, *33*, 811.
- [44] B. D. Vogt, C. L. Soles, H. J. Lee, E. K. Lin, W. Wu, *Polymer* **2005**, *46*, 1635.
- [45] S. Chen, J. Hu, H. Zhuo, *J. Mater. Sci.* **2011**, *46*, 6581.
- [46] T. Pretsch, I. Jakob, W. Muller, *Polym. Degrad. Stab.* **2009**, *94*, 61.
- [47] R. J. Aguerre, C. Suarez, P. E. Viollaz, *Int. J. Food Sci. Technol.* **1989**, *24*, 317.
- [48] C. Liu, H. Qin, P. T. Mather, *J. Mater. Chem.* **2007**, *17*, 1543.

SUPPORTING INFORMATION

Additional Supporting Information may be found online in the supporting information tab for this article.

Fig. S1. Process of moisture absorption testing

Fig. S2. Parameters for moisture-sensitive SME

Fig. S3. the second DSC heating curves of DMAPS/AA copolymers